Climatic Change (2012) 111:249–277
DOI 10.1007/s10584-011-0131-8

A multi-model ensemble of downscaled spatial climate change scenarios for the Dommel catchment, Western Europe

Michelle T. H. van Vliet · Stephen Blenkinsop · Aidan Burton · Colin Harpham · Hans Peter Broers · Hayley J. Fowler

Received: 14 July 2010 / Accepted: 27 May 2011 / Published online: 30 June 2011
© Springer Science+Business Media B.V. 2011

Abstract Regional or local scale hydrological impact studies require high resolution climate change scenarios which should incorporate some assessment of uncertainties in future climate projections. This paper describes a method used to produce a multi-model ensemble of multivariate weather simulations including spatial–temporal rainfall scenarios and single-site temperature and potential evapotranspiration scenarios for hydrological impact assessment in the Dommel catchment (1,350 km^2) in The Netherlands and Belgium. A multi-site stochastic rainfall model combined with a rainfall conditioned weather generator have been used for the first time with the change factor approach to downscale projections of change derived from eight Regional Climate Model (RCM) experiments for the SRES A2 emission scenario for the period 2071–2100. For winter, all downscaled scenarios show an increase in

M. T. H. van Vliet (✉)
Earth System Science and Climate Change, Wageningen University and Research Centre,
P.O. Box 47, 6700 AA Wageningen, The Netherlands
e-mail: michelle.vanvliet@wur.nl

M. T. H. van Vliet · H. P. Broers
Deltares, P.O. Box 85467, 3508 AL Utrecht, The Netherlands

S. Blenkinsop · A. Burton · H. J. Fowler
Water Resource Systems Research Laboratory, School of Civil Engineering and Geosciences,
Newcastle University, Newcastle Upon Tyne, NE1 7RU, UK

C. Harpham
Climatic Research Unit, School of Environmental Sciences, University of East Anglia,
Norwich, Norfolk NR4 7TJ, UK

H. P Broers
TNO Geological Survey of the Netherlands, P.O. Box 80015,
3508 TA Utrecht, The Netherlands

H. P Broers
Department of Hydrology and Geo-Environmental Sciences, VU University,
De Boelelaan 1085, 1081 HV, Amsterdam, The Netherlands

mean daily precipitation (catchment average change of +9% to +40%) and typically an increase in the proportion of wet days, while for summer a decrease in mean daily precipitation (−16% to −57%) and proportion of wet days is projected. The range of projected mean temperature is 7.7°C to 9.1°C for winter and 19.9°C to 23.3°C for summer, relative to means for the control period (1961–1990) of 3.8°C and 16.8°C, respectively. Mean annual potential evapotranspiration is projected to increase by between +17% and +36%. The magnitude and seasonal distribution of changes in the downscaled climate change projections are strongly influenced by the General Circulation Model (GCM) providing boundary conditions for the RCM experiments. Therefore, a multi-model ensemble of climate change scenarios based on different RCMs and GCMs provides more robust estimates of precipitation, temperature and evapotranspiration for hydrological impact assessments, at both regional and local scale.

1 Introduction

There is increasing demand from strategic planners and managers of hydrological systems for detailed information on future climate change and its impacts on water resources. Consequently, there is a need for high resolution climate change scenarios of precipitation, temperature and evapotranspiration to drive hydrological models applied at the local (catchment) or regional (river basin) scale. However, General Circulation Models (GCMs) provide only coarse resolution projections of future climate and so downscaling is required to provide scenarios relevant to hydrological impacts assessments at these scales. Reviews of downscaling methods are provided by Wilby and Wigley (1997), Prudhomme et al. (2002) and, with particular reference to hydrological applications, by Fowler et al. (2007a). In general, downscaling is divided into two approaches: dynamical and statistical downscaling.

Dynamical downscaling uses physically-based Regional Climate Models (RCMs) with boundary conditions provided by a GCM to produce finer spatial scale gridded output and has been used to assess the impact of climate change on hydrological conditions on a European (e.g. Blenkinsop and Fowler 2007; Dankers and Feyen 2009) and regional (e.g. De Wit et al. 2007) scale. Uncertainties in climate model projections (from both GCMs and RCMs) arise not only from alternative scenarios of greenhouse gas emissions, but also due to different representations of large-scale climate processes and the incorporation of the effects of small-scale physics through the parameterization of unresolved processes in climate models. Hence, any climate model simulation may be biased and a given projection represents only one of many possible future climate states. To obtain a representation of alternative possible future climates arising from structural and parameterisation differences between climate models, a multi-model approach (Tebaldi and Knutti 2007) may be used in which a range of different RCMs are considered equally likely (see Fowler et al. 2007a).

Even RCMs are however too coarse for robust hydrological modelling (Fowler et al. 2007a). Therefore, the alternative or additional statistical downscaling approach is generally undertaken. This process encompasses a wide range of different methodologies from relatively simple bias-correction methods to more complex regression-based techniques and weather typing schemes (Wilby and Wigley 1997; Conway and

Jones 1998; Fowler et al. 2007a). Alternatively, stochastic weather generators (Wilby 1999) can be used to produce long time series of simulated weather variables and may be conditioned to simulate future climate by perturbing their parameters or by fitting to perturbed statistics. For example, Semenov and Barrow (1997) perturbed the parameters of a single-site weather generator (LARS-WG) either according to change factors (CFs) derived from GCMs or regressions based on the relationships between coarse resolution GCM grid cell simulations and local-scale observed climate data. Similarly the single-site SDSM model (Wilby et al. 2002) involves applying similar regression relationships to a stochastic weather model. Multi-site downscaling approaches using weather generators are rarer, typically conditioned on weather types and only downscale rainfall (e.g. Charles et al. 2004; Fowler et al. 2005; Cannon 2008). Exceptionally Palutikof et al. (2002) simultaneously downscaled both rainfall and temperature to multi-site locations: a Markov-chain model of wet–dry day state was conditioned on GCM weather types (WTs) for a master site; multi-site rainfall amounts were resampled from observations conditioned on season, WT and wet–dry state; multi-variate estimates of temperature minimum and maximum were predicted from the GCM atmospheric state, conditional on wet/dry state and season.

Haylock et al. (2006) have demonstrated for the UK that the choice of downscaling method introduces a significant source of uncertainty into future projections and that this may vary depending upon the variable and time of year. It is likely therefore that there is no single best downscaling methodology. However, stochastic weather models offer the versatility of being able to generate point, multi-site or spatial weather, including weather that has been previously unseen but that is stochastically similar to the expected control or future climate properties. Additionally, realizations of arbitrary length can be produced, which may be useful for risk analysis related to extreme events.

The catchment of the River Dommel in The Netherlands and Belgium is illustrative of the challenges faced by river basin managers as a consequence of climate change. Previous studies for the River Meuse whose basin includes the Dommel catchment, have indicated that this region may experience an increase in the frequency of short-duration droughts (Blenkinsop and Fowler 2007) and potential decrease in river discharge during the low-flow season (De Wit et al. 2007; van Pelt et al. 2009) whilst extreme discharge in winter may increase (Leander et al. 2008; van Pelt et al. 2009). A number of previous studies have applied the downscaling of climate model projections for hydrological impact assessments of the Meuse. Gellens and Roulin (1998) applied a relatively simple perturbation of baseline climate observations to sub-basins of the Meuse using changes derived from several GCMs. Leander et al. (2008) developed a more sophisticated method using projections from three RCM–GCM configurations, downscaled using a non-linear bias correction method (Leander and Buishand 2007) and a weather generator based on nearest neighbour resampling of climate model output (Leander et al. 2005) to estimate flood quantiles. Booij (2005) assessed the impact of climate change on flooding in the Meuse on a daily basis using generations of a stochastic precipitation model under current and future climate conditions for three GCMs and two RCMs. Output from different GCMs and RCMs in combination with observed precipitation and air temperature series were also used to construct four climate change scenarios (KNMI'06 scenarios) for The Netherlands for the 2050s (2036–2065; Lenderink et al.

2007; van den Hurk et al. 2006). These scenarios project winter (summer) warming of 0.9°C to 2.3°C (0.9°C to 2.8°C) for the 2050s relative to the 1990s (1976–2005), whilst average winter (summer) precipitation amount is projected to change by between +4% to +14% (−19% to +3%) for the whole of The Netherlands.

In this study, a combined stochastic–dynamic downscaling methodology is presented to generate a multi-model ensemble of spatial–temporal rainfall scenarios for the end of the 21st century with consistent temperature and potential evapotranspiration scenarios for hydrological impact assessment in the Dommel catchment. A multi-model approach is followed whereby dynamically-downscaled projections of a future stationary climate time-slice (2071–2100) and control clime time-slice (1961–1990) are provided by eight RCM experiments. Such ensembles are necessary to reflect the uncertainty arising from different climate model structures and parameterization. For hydrological impact assessment of the Dommel catchment, multi-site or spatial rainfall scenarios are required. Therefore the RCM outputs are statistically downscaled using the widely used change factor (CF) approach (Diaz-Nieto and Wilby 2005; Prudhomme et al. 2002) applied to a spatial–temporal stochastic rainfall model (Burton et al. 2008). The traditional application of CFs to observed time series has limitations: future rainfall scenarios can only follow patterns of rainfall previously seen in the observed record; only the rainfall means are changed; changes in the proportion of wet days cannot easily be applied to future projections. However, application of CFs to the proportion of dry days and second or higher moments of the statistics, and use of the projected weather statistics as the basis of parameterising a rainfall model surmounts these problems (see Kilsby et al. 2007; Burton et al. 2010a). This allows the conditional simulation of future spatial–temporal rainfall fields and is the first time that the CF downscaling approach has been applied with a spatial rainfall model. A rainfall conditioned weather generator (Jones and Salmon 1995; Kilsby et al. 2007), perturbed by CFs, is then applied to generate single-site weather time series consistent with the rainfall fields. Stochastic rainfall downscaling to a single site using CFs has recently been applied in the EARWIG (Kilsby et al. 2007), UKCP09 (Jones et al. 2009) and Burton et al. (2010a) approaches. Here, we extend these approaches by applying the CFs derived from RCM experiments to a spatial rainfall model and then using a weather generator to simulate meteorological data consistent with simulated rainfall.

In particular it should be noted that this work improves on the downscaling methodology of Palutikof et al. (2002) in four ways: (1) the single-site discrete-time Markov-chain rainfall occurrence model with multi-site resampling of amounts is replaced with a fully continuous space–time rainfall model which can generate rainfall patterns not previously observed, at locations not used in the calibration and at sub-daily time steps; (2) weather variables in addition to rainfall and temperature (min and max) are generated, making the weather series usable in hydrological studies; (3) a multi-climate-model approach is used; (4) RCMs are used to provide a first step dynamic downscaling of the GCM projections.

This provides the first application of a combined spatial stochastic rainfall model, a rainfall conditioned weather generator and the CF approach to downscale a multi-model ensemble of future climate change scenarios. The provision of an ensemble of downscaled future weather series, including spatially distributed rainfall, will enable concerns over the effect of climate change on local hydrology, the leaching of heavy metals and surface water quality to be investigated in this region (Visser et al. 2011).

2 The Dommel catchment: meteorological data and climate models

2.1 Geographical context and meteorological data of the Dommel catchment

The study area comprises the catchment of the River Dommel, a tributary of the Meuse (Fig. 1) on the Belgium–Dutch border. It has a total area of 1,350 km^2 with a low lying elevation ranging from 5 m to 76 m above sea level. The Dommel drains an intensive agricultural and densely populated area of approximately 593,000 people. The soils, riverbed and water of the Dommel are heavily contaminated with zinc and cadmium as a result of the historical pollution of the area by a nearby zinc smelter (De Jonge et al. 2008) making this catchment an important hydrological case study in terms of future water supply and quality.

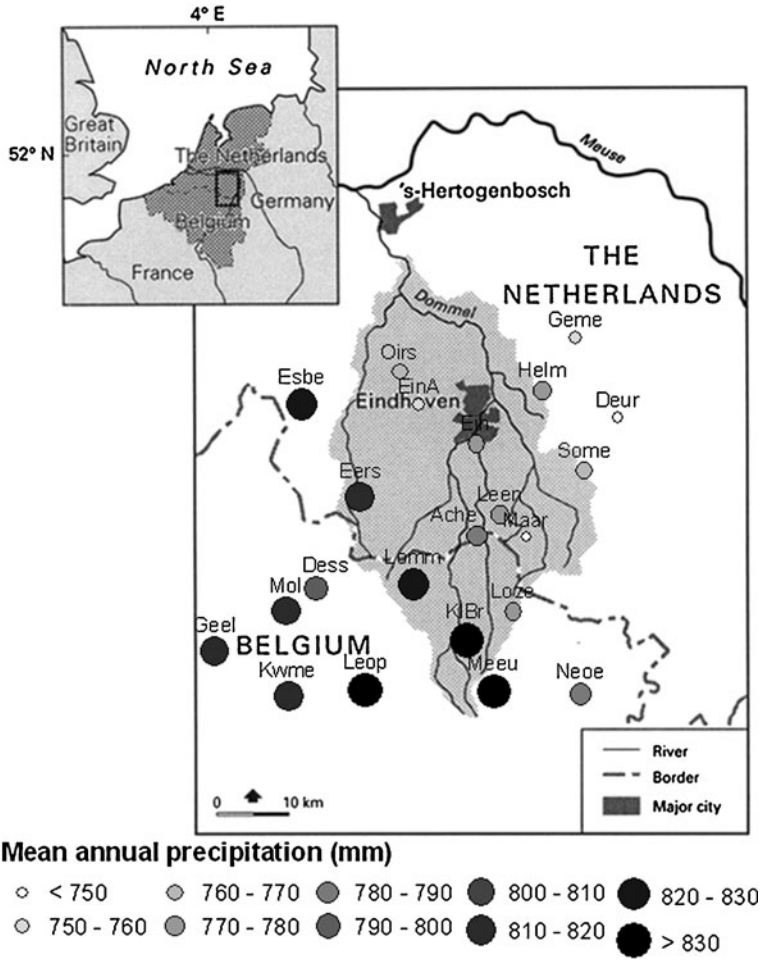

Fig. 1 The Dommel catchment (based on Pieterse et al. (2003) with permission from Elsevier), location of precipitation stations and annual precipitation averaged over the period 1961–1990. Abbreviated meteorological station names are used (for details see Table 1)

The climate of the Dommel region is temperate, with relatively cool summers and mild winters. A total of 22 meteorological stations are located within the study area of the Dommel catchment (Fig. 1). For this study, daily precipitation data for the period 1961–1990 for the 11 gauges located in Belgium were provided by the Royal Meteorological Institute of Belgium (KMI-RMI), whilst the precipitation series of the 11 Dutch gauges were obtained from the Royal Netherlands Meteorological Institute (KNMI). Additional time series of daily minimum and maximum temperature, sunshine duration, vapour pressure and wind speed were obtained from KNMI for the station at Eindhoven. This station was selected because it offers a longer continuous series of homogeneous climate data (1985–2006) than is available elsewhere.

Average mean annual precipitation across all gauges is 792 mm (over the period 1961–1990) and ranges from 747 mm (Maarheze) to 838 mm (Leopoldsburg and Meeuwen), generally increasing from north-east to south-west (Fig. 1; Table 1). The annual cycles of temperature and precipitation are shown in Fig. 2. This indicates that daily mean precipitation at Eindhoven, located in the centre of the study area (Fig. 1), is comparable with the overall average of all 22 stations.

Potential evapotranspiration (PET) is estimated using the Penman–Monteith method (FAO 1986) by applying the daily series of air temperature (minima and maxima), wind speed, vapour pressure and sunshine hours for Eindhoven. The annual mean PET is estimated at 673 mm (over the period 1985–2006) with a strong seasonal cycle with highest values during July (3.6 mm/day; Fig. 2).

Table 1 Characteristics of selected precipitation stations in the study area where country is indicated as either BE (Belgium) or NL (the Netherlands)

Identifier	Station name	Latitude (degrees)	Longitude (degrees)	Altitude (m)	Annual precipitation (mm; 1961–1990)	Country
Ache	Achel	51.30	5.48	26	781	BE
Dess	Dessel	51.23	5.16	28	800	BE
Deur	Deurne	51.27	5.46	22	750	NL
Eers	Eersel	51.21	5.15	29	820	NL
Ein	Eindhoven	51.25	5.29	18	773	NL
EinA	Eindhoven Airport	51.28	5.22	20	754	NL
Esbe	Esbeek	51.28	5.08	21	826	NL
Geel	Geel	51.16	4.96	18	816	BE
Geme	Gemert	51.33	5.41	17	754	NL
Helm	Helmond	51.29	5.37	20	773	NL
KlBr	Kleine Brogel	51.17	5.46	64	836	BE
Kwme	Kwaadmechelen	51.10	5.11	29	815	BE
Leen	Leende	51.20	5.32	26	779	NL
Leop	Leopoldsburg	51.11	5.26	48	838	BE
Lomm	Lommel	51.24	5.36	44	826	BE
Loze	Lozen	51.21	5.56	36	772	BE
Maar	Maarheeze	51.18	5.35	28	747	NL
Meeu	Meeuwen	51.11	5.52	71	838	BE
Mol	Mol	51.21	5.10	23	812	BE
Neoe	Neeroeteren	51.10	5.69	44	786	BE
Oirs	Oirschot	51.30	5.20	15	770	NL
Some	Someren	51.23	5.42	29	761	NL

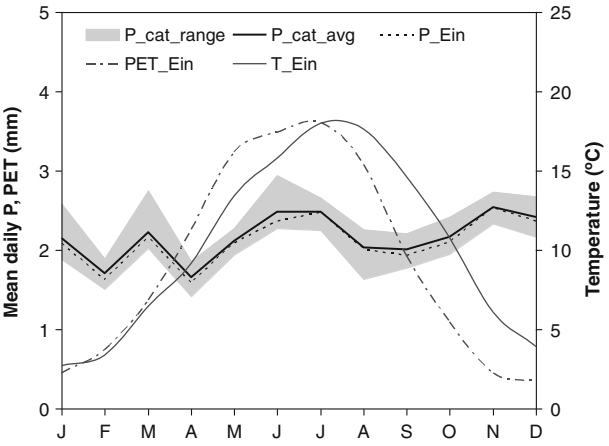

Fig. 2 Average (*P_cat_avg*) and range (*P_cat_range*) of mean daily precipitation for the Dommel catchment and mean daily precipitation (*P_Ein*), potential evapotranspiration (*PET_Ein*) and air temperature (*T_Ein*) for station Eindhoven for each month over the period 1985–2006

2.2 Climate models

One way of addressing the uncertainties in climate model simulations noted in Section 1 is through the use of multi-model ensembles. Therefore, projections of future changes in climate over the Dommel were derived using Regional Climate Model (RCM) output from the European Union Fifth Framework Programme (FP5) PRUDENCE project (Christensen et al. 2007). This project used RCMs to provide a series of high-resolution simulations of European climate through "time-slice" experiments, generating stationary climate simulations for control (1961–1990) and future (2071–2100) time periods. Each RCM derives its boundary conditions from, and so dynamically downscales, a GCM. Here, the output of eight PRUDENCE RCM experiments was utilized (Table 2) using six different RCMs (for further details on RCM formulations see Jacob et al. (2007)) and two groups of GCMs. The

Table 2 The eight Regional Climate Model (RCM) experiments used from the FP5 PRUDENCE project

Aquaterra acronym	RCM	Driving GCM	Prudence acronym (control/future)
HIRHAM_H	HIRHAM	HadAM3H A2	HC1 / HS1[a]
HIRHAM_E	HIRHAM	ECHAM4/OPYC A2	Ecctrl / ecscA2
RCAO_H	RCAO	HadAM3H A2	HCCTL / HCA2
RCAO_E	RCAO	ECHAM4/OPYC A2	MPICTL / MPIA2
HAD_P_H	HadRM3P	HadAM3P A2	adeha / adhfa
ARPEGE_H	Arpège	HadCM3 A2	DA9 / DE6
RACMO_H	RACMO	HadAM3H A2	HC1 / HA2
REMO_H	REMO	HadAM3H A2	3003 / 3006

The acronyms from the FP6 AquaTerra (integrated modeling of river-sediment-soil-groundwater system for management of catchments in the context of global change) project (Barth et al. 2009) are used throughout this paper. The suffix of each denotes the driving General Circulation Model (GCM). The equivalent PRUDENCE acronyms are provided for information

[a]One member from a 3-member ensemble has been used for these RCMs

selected experiments duplicate the choice of RCM with different GCMs, allowing some comparison of the influence of the choice of GCM and RCM. However, the full range of uncertainty generated by the choice of GCM boundary conditions is necessarily constrained by the experimental structure provided by the PRUDENCE project (Déqué et al. 2007). Boundary conditions in this ensemble are thus derived primarily from HadAM3H (Pope et al. 2000) and ECHAM4/OPYC (Roeckner et al. 1996). The HadRM3P and ARPEGE RCM simulations derive boundary conditions from HadAM3P and HadCM3 respectively. Both HadAM3H and HadAM3P are dynamically downscaled to an intermediate resolution from HadCM3 and are thus closely related and may be considered as the same GCM.

3 Methodology

3.1 Multi-site daily precipitation timeseries: the Spatial–Temporal Neyman–Scott Rectangular Pulses model

Poisson cluster models were first described for rainfall modelling by Le Cam (1961) and have the useful property that they can generate continuous spatial–temporal random fields (e.g. Gupta and Waymire 1979) which is increasingly relevant for distributed hydrological modelling applications. The Neyman–Scott Rectangular Pulses model (NSRP; Rodriguez-Iturbe et al. 1987) is a single-site rainfall time series model based on the Poisson cluster approach whereby storms occur with a Poisson process in time. Each storm origin creates a random cluster of raincells each of which provides a 'rectangular pulse' of rainfall with an intensity and a duration. A spatial version of this model, the Spatial–Temporal Neyman–Scott Rectangular Pulses (STNSRP) model (Fig. 3), which is suitable for simulations of up to ~200 km in diameter, was formulated by Cowpertwait (1995). A recent implementation of the STNSRP model is provided by Rainsim V3 (Burton et al. 2008), which is capable of simulating rainfall either spatially or for a single location at hourly or daily time steps and which has been used in a broad range of climates and end-user applications. The spatial, rather than the simpler multi-site, simulation properties of this model were recently demonstrated by Burton et al. (2010b) by validating simulations of rain gauges at locations that were not used in model calibration. Here, however, only the model's multi-site properties are utilised.

In the STNSRP stochastic conceptualization of rainfall (Fig. 3; Cowpertwait 1995; Burton et al. 2008) a temporal sequence of storm origins each gives rise to a set of raincell events that occur as a stationary Poisson process in space. The raincells are clustered in time following the storm origin, and each has intensity and duration properties. Time series of rainfall accumulations may be sampled from the process by aggregating the contributions of all active raincells over each time interval at any location. The sum of the intensities of all active raincells is scaled by a nonhomogeneous spatial intensity field which is calculated in proportion to the mean daily rainfall amount (further details may be found in Burton et al. 2010b). The stochastic model structure is shown in Fig. 3 and Table 3 summarises the model parameters. An annual cycle of rainfall properties is obtained by using different parameterizations for each calendar month.

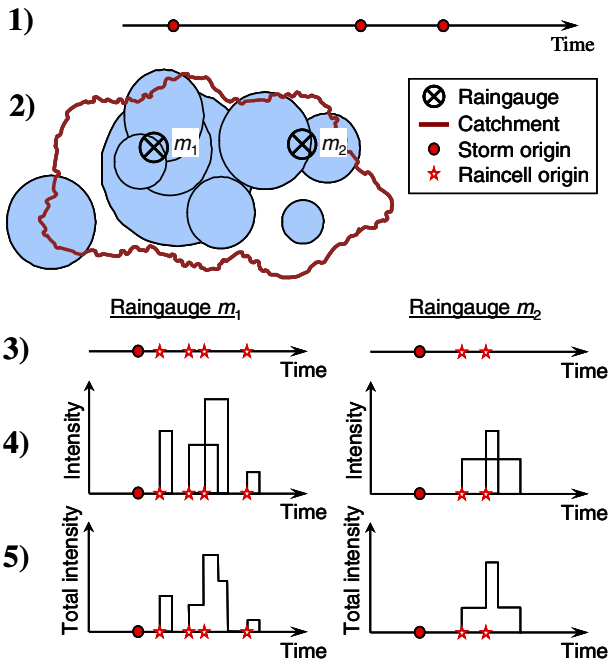

Fig. 3 Schematic of the Spatial–Temporal Neyman–Scott Rectangular Pulses (STNSRP) stochastic rainfall model's process. (*1*) Storm origins occur as a Poisson process in time. (*2*) Each storm origin generates a set of circular raincells whose centres occur as a spatial Poisson process and each with an exponentially distributed radius. The subsequent temporal development of the model is then shown as if sampled at the locations of two raingauges m_1 and m_2. (*3*) Each raincell starts at a time-origin which follows the storm origin after an exponentially distributed time interval. (*4*) Each raincell produces rainfall with a uniform intensity across its disc and throughout its lifetime. The duration and the intensity of each raincell is exponentially distributed. (*5*) The spatial rainfall intensity field is the sum of the intensities of all the active raincells scaled by a non-uniform spatial intensity field. Parameters of the process are given in Table 3

Table 3 Monthly varying parameters of the Spatial–Temporal Neyman–Scott Rectangular Pulses (STNSRP) model and the associated procedure for sampling each corresponding random variable (RV)

Parameter	Description	Unit	Sampling
λ^{-1}	Mean waiting time between adjacent storm origins	(h)	Exponential RV
β^{-1}	Mean waiting time for raincell origins after storm origin	(h)	Exponential RV
η^{-1}	Mean duration of raincell	(h)	Exponential RV
ξ^{-1}	Mean intensity of a raincell	(mm/h)	Exponential RV
γ^{-1}	Mean radius of raincell	(km)	Exponential RV
ρ	Spatial density of raincell centres	(km^{-2})	Spatial Poisson process
$\psi(\mathbf{x})$	Non homogeneous intensity scaling field for all points, $\mathbf{x}$, in the simulation region	(–)	–

Properties of the simulated rainfall exhibit high sample variability and so would require excessive computation to determine with precision. Instead expected properties of the model, calculated from analytical expressions, are used in the fitting. Thus the model is fitted using a numerical optimization scheme to identify the parameters that minimize an objective function which compares the expected properties of the stochastic simulation process to a selected set of observed rainfall statistics. This comparison depends on the availability of analytical expressions that estimate expected simulation properties as functions of the model parameters. Such expressions are available for arbitrary locations and aggregation periods for the mean, variance, lag-autocovariance, lag-autocorrelation, dry period probability, probability of dry–dry (or wet–wet) transitions, third order central moment and skewness coefficient (e.g. Cowpertwait 1995, 1998). Expressions for the cross-covariance and cross-correlation between two locations are also available (Cowpertwait 1995) and are useful to characterise the model's spatial properties. RainSim V3 (Burton et al. 2008) further facilitates the fitting procedure with a highly efficient optimizing algorithm, a new objective function that reduces problems arising from preferential fitting of observed statistics and a reduction in the fitting biases of the dry-period probability.

3.2 Daily temperature and evapotranspiration series: the CRU weather generator

The Climatic Research Unit (CRU) daily weather generator (hereafter abbreviated to CRU-WG) was initially developed by Jones and Salmon (1995). In the initial implementation daily rainfall series were generated using a two state Markov chain model; however a recent development (Kilsby et al. 2007) has been to replace this rainfall model with a single-site NSRP stochastic rainfall generator and to use this to condition a modified version of the CRU-WG developed by Watts et al. (2004a). This approach offers improved reproduction of extremes and may be explicitly re-parameterised using projected future statistics from RCMs.

The CRU-WG uses a cascade of regressive and auto-regressive relationships, fitted to point observations of meteorological data, to generate long time series of synthetic daily weather variables. The primary weather variable in this model is rainfall which here is taken from the multi-site rainfall dataset simulated in Section 3.1. Since the CRU-WG is a single-site model the rainfall series (P) simulated for Eindhoven (see Section 2.1; Fig. 1) was used to condition the simulation of the additional weather variables which are considered to be representative of the Dommel catchment. This location was selected as it has the best historic record for the catchment including the input variables of daily temperature maxima (TX), temperature minima (TN), vapour pressure (VP), wind speed (WS) and sunshine hours (SS). In the CRU-WG secondary variables (Table 4) are simulated using the regressive and auto-regressive relationships with further variables calculated from these.

The weather generator calculates daily mean temperature (T) and daily temperature range (TR) by a first-order auto-regressive process incorporating the lag-1 daily mean temperature, temperature range and precipitation, the latter dependent on conditioning by four daily rainfall transition states (dry–dry, wet–wet, dry–wet and wet–dry) as described in Kilsby et al. (2007). TN and TX are subsequently derived from the relationships $TN = T - 0.5\ TR$ and $TX = T + 0.5\ TR$. The variables VP,

Table 4 List of weather variables generated by the Climatic Research Unit weather generator (CRU-WG)

Variable and category	Symbol
(1) Primary variable	
Precipitation (mm)	*P*
(2) Secondary variables	
Mean temperature (°C)	*T*
Daily temperature range (°C)	*TR*
Vapour pressure (hPa)	*VP*
Wind speed (ms^{-1})	*WS*
Sunshine duration (hours)	*SS*
(3) Calculated variables	
Relative humidity (%)	*RH*
Reference PET ($mm\ day^{-1}$)	*PET*

The primary variable (1) is precipitation which is generated using the STNSRP model. Secondary variables (2) are simulated by the CRU-WG which also calculates further variables (3) from these

WS and *SS* are then determined by regression analyses incorporating *P* and *T*. The regression form maintains the autocorrelation structures of these variables and preserves correlations with both *T* and *P*. Furthermore, observed correlations between these three variables also arise naturally due to their common dependency on *T* and *P*. Finally, the simulated variables are used to calculate potential evapotranspiration (PET) using the Penman–Monteith method (FAO 1986). Further details of the implementation of the CRU-WG and details of validation experiments are presented in Kilsby et al. (2007) and Watts et al. (2004a, b), and its application in the production of the state-of-the-art UK Climate Projections (UKCP) is described by Jones et al. (2009).

3.3 Deriving change factors from regional climate models

For each of the eight selected RCM experiments from the PRUDENCE project (Section 2.2; Table 2), simulated values of mean daily temperature and daily total precipitation for the 1961–1990 (control) and 2071–2100 (scenario) time-slices were extracted from the two RCM grid cells overlying the meteorological stations in the study area (Fig. 1). Because the approach applies CFs to observed climate statistics an explicit bias correction of the RCM output is unnecessary although it assumes, as with bias correction, that model biases are consistent in control and future simulations. For each grid cell monthly change factors (CFs) for mean daily rainfall, proportion of dry days (PDD; defined as days with less than 1.0 mm of rainfall), daily rainfall variance, daily rainfall skewness (SKEW) and daily lag-1 auto correlation (AC) were calculated. For air temperature, monthly CFs of mean and variance in daily temperature were derived. The CF approach (Diaz-Nieto and Wilby 2005; Prudhomme et al. 2002) assumes that future changes to local rainfall statistics will be proportional to changes simulated by an RCM. The approach of our study extends the approach of Kilsby et al. (2007), who used CFs from a single climate model (HadRM3H), by using a multi-model ensemble, and by the application of the approach to a spatial multi-site rather than single-site rainfall model.

Following the approach described in Kilsby et al. (2007) and Jones et al. (2009), change factors, $\alpha^{R}_{g,i}$ (Eq. 1), were calculated to measure the change in each rainfall

statistic, g, for each RCM, R, between the control (*Con*) and future (*Fut*) time-slices for each calendar month, i, for the two grid cells overlying the Dommel catchment.

$$\alpha_{g,i}^{R} = \frac{g_i^{R,Fut}}{g_i^{R,Con}} \tag{1}$$

Estimates of future rainfall statistics, $g_i^{R,Est}$, based on change factors from each RCM and from statistics observed during the control period (*Obs*), g_i^{Obs}, were then obtained using Eq. 2.

$$g_i^{R,Est} = \alpha_{g,i}^{R}\, g_i^{Obs} \tag{2}$$

Changes in daily temperature variance may also be calculated in the same way, however, PDD and AC statistics take values within limited ranges and so they were first transformed using simple invertible transformations (see Burton et al. 2010a), prior to evaluating or applying CFs. Estimates of future PDD and AC may then be calculated as for other rainfall statistics by using an appropriate application of the change factor. A detailed description of this process is provided in the annex of Jones et al. (2009).

For mean temperature, T, change is additive and so the change factor is derived from RCM simulations using Eq. 3 and used to perturb future monthly mean temperature through the application of Eq. 4. The daily temperature variance is also perturbed by the ratio of the future to the control variance from the RCM in the same way as for mean precipitation shown in Eqs. 1 and 2 (see Kilsby et al. 2007). The CRU-WG then provides simulations of daily temperature with the properties of the perturbed statistics in the same way as described in Section 3.2.

$$\alpha_{T,i}^{R} = T_i^{R,Fut} - T_i^{R,Con} \tag{3}$$

$$T_i^{R,Est} = T_i^{Obs} + \alpha_{T,i}^{R} \tag{4}$$

In this study, an additional correction to the CFs is necessary as the period of observed data for temperature and the other CRU-WG variables (1985–2006) is not concurrent with the RCM control time-slices (1961–1990) and may therefore be assumed to include a proportion of the change projected by the RCMs. A simple pattern scaling approach, described by Burton et al. (2010a) was therefore applied to the CFs to rebase them to the observation period by assuming that changes in monthly temperature statistics are proportional to global mean temperature throughout the period between the control and future time-slices. Pattern scaling (Santer et al. 1990; Mitchell 2003) has been widely used to produce scenarios for stationary time-slices not covered by GCM/RCM simulations and has been shown to be generally accurate for temperature and precipitation change at seasonal and grid scales (Mitchell 2003; Tebaldi et al. 2004). The scale factor rebasing method described by Burton et al. (2010a) was adapted here for temperature rebasing. The rebasing of these weather statistics was estimated using projections of global mean temperature from the GCMs HadCM3 and ECHAM4, scaling according to which was used to condition each of the eight RCM experiments (Table 2). Further details of the pattern scaling approach used here are given in Appendix 1.

For each of the eight RCM experiments the set of seven CFs (five for precipitation, two for temperature) relative to the period for which observed data was available was calculated for each calendar month, resulting in a total of 84 (7×12) estimates of future monthly weather statistics. In numerical models such as RCMs, the limits to process integration and numerical instabilities at the grid scale mean that projections for individual RCM grid cells must be treated with caution. CFs for a 12 (4×3) element grid centred on the two grid cells for the Dommel were examined to ensure that the RCMs provided regional spatial consistency.

Across the 12 element grid the range in monthly CFs for mean precipitation is typically around 10% although there is some model variability. For example, for HIRHAM_E the range is only ~6% whilst for HAD_P_H it is typically ~13%. This spatial variability tends to be smallest in summer with little variation across the domain whilst in some models it is larger in winter and spring months with a weak pattern of larger increases in the north. For mean temperature the range in monthly CFs for most models is generally < 0.5°C and in the case of RACMO_H, REMO_H and ARPEGE_H is generally < 0.2°C. For most models the range is greatest during summer months, particularly HIRHAM_E (1.6°C, August) and RCAO_E (2.3°C, August). This enhanced summer range is, in general terms associated with greater temperature increases in the south. It was concluded that the CFs derived from each of the RCMs are spatially consistent and that the grid cells overlying the Dommel were therefore appropriate for this study. The final set of CFs used in this study was subsequently derived as an average of the two grid cells.

Figure 4 illustrates the projected average CFs calculated from the RCMs for the grid cells corresponding to the Dommel for mean precipitation and temperature. The projected changes are discussed in more detail in Section 5 in the context of the downscaled climate change scenarios. However, in general terms, mean precipitation is projected to increase between December and March ($CF > 1$) and decrease between May and September ($CF < 1$). All RCMs project temperature increases throughout the year but especially during summer.

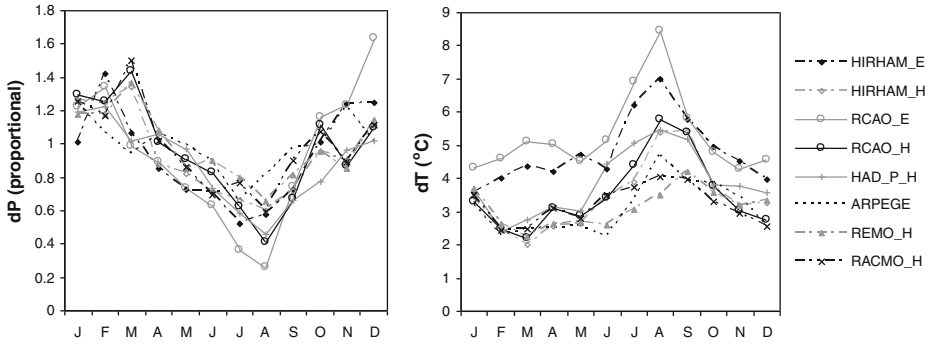

Fig. 4 **a** Multiplicative change factors of mean precipitation and **b** additive change factors of mean temperature, for the eight selected Regional Climate Model (RCM) experiments averaged over the two grid cells overlying the meteorological stations in the Dommel catchment

4 Results of control climate simulations

4.1 Validation of the STNSRP model: control simulations

The daily rainfall observations for the control period, 1961–1990, for the 22 selected rain gauges were used to calibrate the STNSRP model. This calibration was subsequently used to generate a 100-year climatically stationary simulation for the control period at the rain gauges' locations (i.e. using only the multi-site properties of the model). To achieve this, each rain gauge record was first characterized in terms of calendar month estimates of the daily mean, variance, PDD, AC and SKEW statistics. The daily cross-correlation between the rain gauges was also evaluated for each calendar month making a total of 4092 observed statistics (12 calendar months $\times$ [22 $\times$ 5 single-site statistics + 231 cross-correlation statistics]). An STNSRP model parameter set was then fitted for each calendar month using numerical optimization and a 100-year daily spatial simulation of the model was generated and sampled at the locations of the 22 rain gauges.

Analysis of the simulated time series provides a demonstration that the model outputs are consistent with the characteristics of the observed rainfall. The observed, fitted and simulated monthly statistics of the control simulation are presented in Fig. 5 for five of the precipitation stations: Maarheeze (Maar), Deurne (Deur), Eindhoven (Ein), Eersel (Eers) and Leopoldsburg (Leop). These stations were selected to represent the range of precipitation amounts in the catchment from the lowest to highest annual amounts (Fig. 1). Both fitted and simulated monthly statistics are presented, which are slightly different due to the stochastic nature of the simulations: fitted values are those expected from the rainfall model and simulated values exhibit sample variability. The spatial rainfall cross-correlation properties are shown in Fig. 6 for pairs of the 22 stations for January and July.

The differences between the observed precipitation properties of the selected stations are fairly small due to the small altitudinal range of the catchment and its uncomplicated topographic setting. The cross-correlation properties exhibit more localised (less spatially correlated) events in the summer than the winter (as illustrated in Fig. 6), reflecting an annual cycle between smaller (e.g. convective) and larger (e.g. stratiform) rainfall systems. Model fits to the observations are generally good, indicating that the model provides a good structural match to the observed rainfall. In particular, fits to mean and PDD were found to be good for all 22 rainfall gauges. Overall, the properties of the simulation are seen to approximate the fits, with some variation arising from the stochastic nature of the simulation. Although fits and simulations of SKEW are somewhat underestimated for the stations of Eindhoven and Maarheeze during summer, the majority of stations are well simulated in terms of this statistic, which is highly susceptible to sample variability. For most months, the spatial properties are very well fitted with the possible exception of May to July which appears to exhibit a slight under-simulation of the correlation for distances greater than about 50 km (July shows the worst example of this in Fig. 6). However, observed data for May and June appear to show an increasing correlation with distance for distances greater than about 50 km and August has the least correlation at ~60 km (and is accurately simulated). Therefore it is likely that much of this difference arises from sample variability. In general, the synthetic data series are found to provide a good representation of rainfall observed simultaneously at the 22 rainfall stations in the study area for the control period.

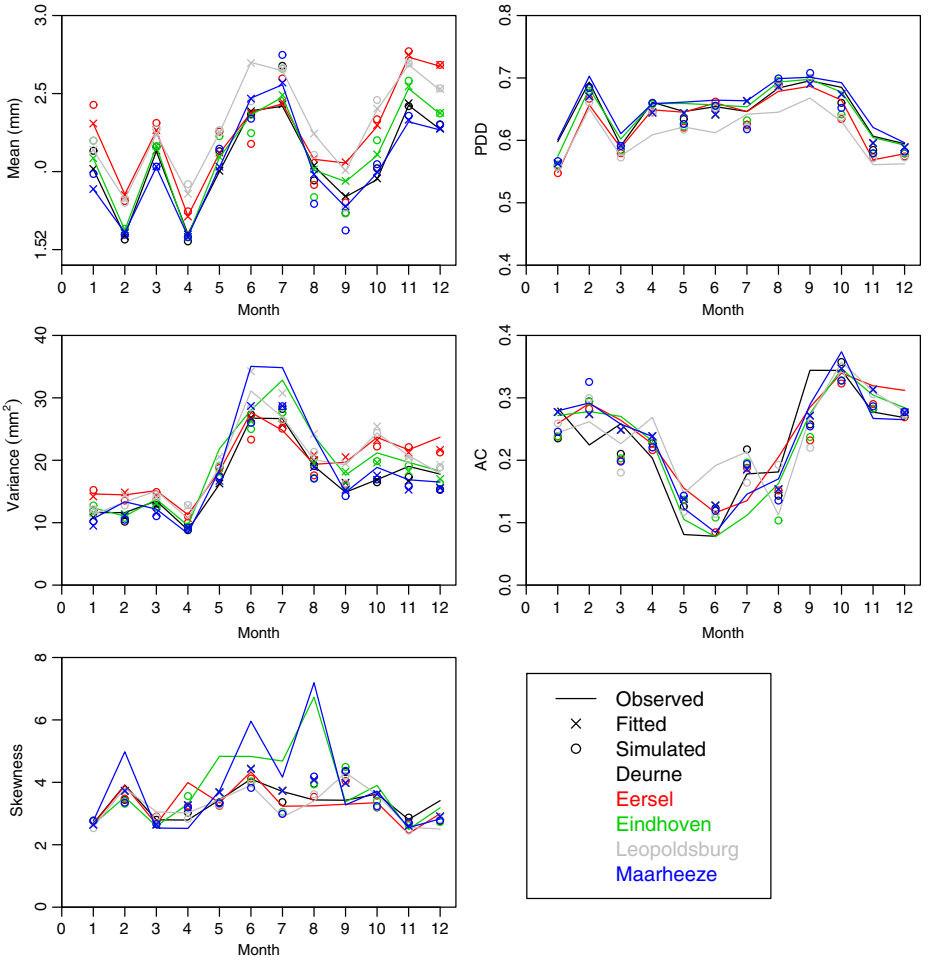

Fig. 5 Observed, fitted and simulated monthly statistics of **a** mean daily rainfall, **b** proportion of dry days (PDD), **c** daily variance, **d** daily lag-1 autocorrelation (AC), **e** daily skewness coefficient (SKEW), for the five stations in the Dommel catchment with each *colour* representing one site

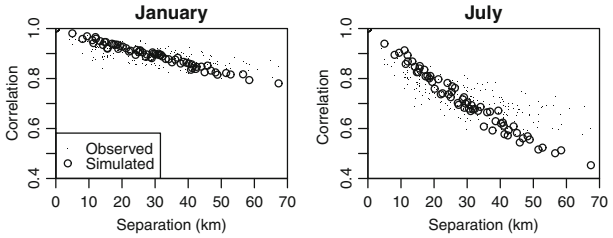

Fig. 6 Observed (*points*) and simulated (*circles*) cross-correlations against station separation for January and July. All 231 possible pairs of rainfall stations in the Dommel catchment, are shown for the observed and a sub-sample for simulated points

4.2 Validation of the CRU weather generator: simulations for the weather observation period

As previously noted, the CRU-WG is currently only developed as a single-site application and so cannot be used to produce spatially correlated series of the additional weather variables in the same manner as the STNSRP model is able to simulate for precipitation. However, Jones et al. (2009) suggests that the approach may be appropriate for catchments of up to approximately 1000 km^2. In practice, simulating these variables at a single point is sufficient for hydrological modelling of the Dommel due to the relatively low spatial variability of temperature and potential evapotranspiration over the catchment arising from its limited size and homogeneous nature. Correlation in mean daily air temperature between the meteorological stations in the Dommel catchment ranges from 0.980 to 0.997. As discussed in Sections 2.1 and 3.2, Eindhoven was selected as the most appropriate station to provide representative meteorological data because it offers the longest complete record (1985–2006), it is centrally located, its precipitation is close to the catchment

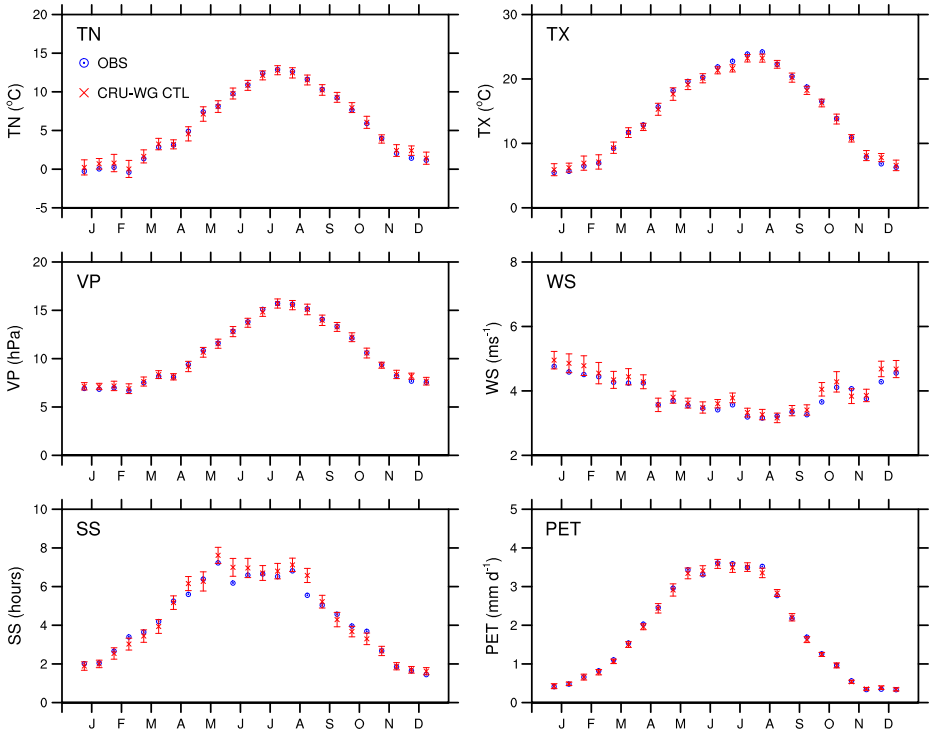

Fig. 7 Validation of Climatic Research Unit weather generator (*CRU-WG*) for simulated daily temperature minima (*TN*), and maxima (*TX*), vapour pressure (*VP*), wind speed (*WS*), sunshine hours (*SS*) and potential evapotranspiration (*PET*) for the weather observation (*WObs*) period (1985–2006). The *crosses* denote the CRU-WG simulated means of weather statistics for the *WObs* period (*CRU-WG CTL*) and the *circles* show the corresponding observed values (*OBS*). The *error bars* represent variability denoted by two standard deviations of the simulated 100 annual means

average (Fig. 2) and the record length is sufficient to produce reliable calibrations (Watts et al. 2004a). The CRU-WG was therefore calibrated on the Eindhoven data.

To validate the CRU-WG an assessment of its ability to adequately simulate the main features of the observed climate at Eindhoven was undertaken. As the regression relationships used by the CRU-WG are dependent on rainfall state and amount, simulated rainfall series (Section 4.1) characterised by monthly mean estimates of the daily mean, variance, PDD, AC and SKEW statistics of rainfall, estimated for the weather observation (*WObs*) period (1985–2006) from the Eindhoven meteorological station were used to condition the CRU-WG to generate 100 30-year *WObs* simulations of the observed weather.

The performance of the CRU-WG in reproducing the mean climatology at Eindhoven is assessed in Fig. 7, by comparing the observed average weather statistics with the range estimated from the 100 simulations. This shows that the weather generator skilfully reproduces both *TN* and *TX* throughout the year with the observed average within the two standard deviation range of the simulations for most half-months of the year. Only during summer is there a slight underestimation of *TX* by the CRU-WG, with the observed means outside the range of two standard deviations of the simulations. For *VP*, *WS* and *SS* there is close correspondence between the observed and simulated values throughout the year although *WS* is overestimated for some half monthly periods whilst the same is true for *SS* during spring and summer periods. Overall, the simulations show excellent agreement with observed values and reproduce the annual cycles of all weather variables well. Of particular importance to hydrological assessment, the PET simulations display a close correspondence with observed values throughout the year.

5 Results of future climate simulations

5.1 Future projections of multi-site precipitation

The projected statistics of future multi-site rainfall were estimated using the CF approach described in Section 3.3 for each raingauge and RCM experiment. The STNSRP model was then fitted to these statistics for each of the eight RCM experiments in turn and used to generate daily 100-year stationary-climate time series of precipitation for all stations for the future (2071–2100) time-slice corresponding to the projections of each of the RCMs.

Roughly, the downscaled time series of future precipitation for the RCM experiments project an increase in winter precipitation and a decrease in summer precipitation, which is in agreement with the CFs of the selected RCM projections (Section 3.3; Fig. 4). Figure 8 shows the mean daily precipitation for the driest station Maarheeze and wettest station Leopoldsburg, which are indicative of the spatial range, and the overall average in mean daily precipitation of all 22 raingauges (catchment average) for the 100-year simulations of the future period (2071–2100) compared to the control period (1961–1990). Comparing the magnitude and timing of the downscaled multi-site precipitation, distinct differences exist between the selected RCMs. The most pronounced increases in winter precipitation and decreases in summer precipitation are obtained for RCAO_E, while seasonal precipitation changes for ARPEGE_H are less obvious compared to the other RCMs. This is

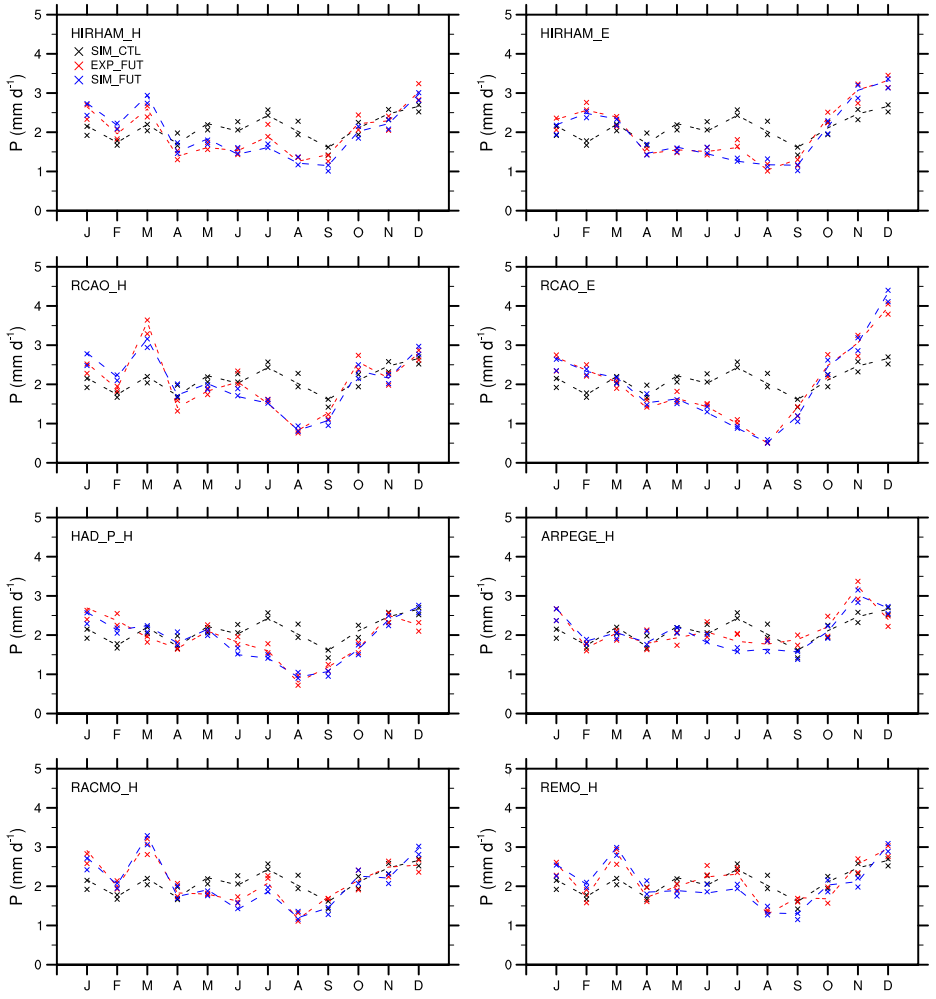

Fig. 8 Mean daily precipitation of the driest station (Maarheeze) and wettest station (Leopoldsburg) and the overall average of all 22 raingauges (catchment average) for the eight 100-year simulations of the future period (2071–2100) compared to the control period (1961–1990). The values of the driest and wettest stations are presented for the control (SIM_CTL; *black crosses*), simulated future (SIM_FUT; *blue crosses*) and expected future (EXP_FUT; *red crosses*) periods and the dotted lines denote the overall catchment averages of mean daily precipitation

in agreement with the calculated CFs (Fig. 4). Precipitation projections based on RCAO_H show a distinct emphasising of the precipitation peak during March for all sites, which is (to a lesser extent) also found for the HIRHAM_H, REMO_H and RACMO_H precipitation simulations. Comparing the HIRHAM and RCAO experiments using boundary conditions from two different GCMs (HadAM3H and ECHAM4/OPYC; suffix _H and _E respectively) suggests that the increased precipitation peak during March derives from the driving GCM, since the increase in precipitation during this month is only found for the experiments using boundary conditions from HadAM3H.

For winter (DJF), all downscaled scenarios show an increase in catchment average daily mean precipitation and standard deviation (SD), and typically an increase in the proportion of wet days (P_{wet}; P > 1.0 mm) is indicated (Table 5). The increase in mean daily precipitation spans a wide range between +9% (ARPEGE_H) and +40% (RCAO_E). There is a strong suggestion that the GCM influences the winter wet-day amount (M_{wet}) as both HIRHAM_E and RCAO_E exhibit greater increases than their HadAM3H-driven counterparts. Changes in M_{wet} during winter are also highest for RCAO_E (+23%), while less pronounced increases in mean daily precipitation and M_{wet} are projected for RCAO_H (+19% and +4% respectively), indicating that GCM boundary conditions strongly influence the precipitation increases. However, the highest increases in the proportion of wet days (P_{wet}) were found for HIRHAM_H (+22%) while the run based on RACMO_H resulted in a very small overall average decrease in P_{wet} during winter (−1%).

For summer (JJA), all scenarios show a decrease in mean daily precipitation ranging from −16% (REMO_H) to −57% (RCAO_E), an increase in CV and a decrease in P_{wet} from 26% (ARPEGE_H and REMO_H) to 62% (RCAO_E). Typically the overall catchment average of M_{wet} is projected to increase during summer; by up to 16%. This suggests that the projected reduction in summer rainfall arises despite an intensification of rainstorm events due to a greater decrease in P_{wet}. The projected changes in daily summer precipitation for the RCM experiments HIRHAM_E and RCAO_E result in more pronounced drier conditions than found with HIRHAM_H and RCAO_H: greater decrease in the mean, higher increase in CV and greater decrease in P_{wet} with inconclusive results for M_{wet}. This suggests that the GCM boundary conditions strongly influence changes in precipitation during summer principally through the mechanism of reducing the number of wet days.

5.2 Future projections of mean temperature and evapotranspiration

To generate consistent future scenarios of temperature and other weather variables, the CFs associated with each of the eight RCM simulations were used to produce the future climate simulations as described in Section 3.3. As the CRU-WG generates the weather variables in a specific sequence for three groups of variables (Table 4) the perturbations are modified to allow for changes that have arisen earlier in this

Table 5 Catchment average percentage change in mean, standard deviation (st.dev), coefficient of variation (CV), proportion of wet days (P_{wet}: P > 1.0 mm) and mean wet day amount (M_{wet}) during winter (DJF) and summer (JJA) for the eight Regional Climate Model (RCM) experiments

	HIRHAM_H	HIRHAM_E	RCAO_H	RCAO_E	HAD_P_H	ARPEGE_H	RACMO_H	REMO_H
Changes (%) Winter (DJF)								
mean	+19	+18	+19	+40	+13	+9	+14	+13
st.dev	+2	+25	+14	+39	+20	+11	+2	+6
CV	−14	+6	−5	−1	+6	+2	−11	−6
P_{wet}	+22	+5	+15	+15	+2	−1	+15	+10
M_{wet}	−2	+12	+4	+23	+10	+11	−1	+3
Changes (%) Summer (JJA)								
mean	−35	−39	−35	−57	−39	−19	−31	−16
st.dev	−16	−7	+4	−24	−2	−3	+3	+17
CV	+29	+54	+60	+78	+62	+21	+49	+39
P_{wet}	−35	−45	−44	−62	−45	−26	−40	−26
M_{wet}	−1	+9	+15	+11	+8	+9	+16	+11

Changes are expressed for the future period (2071–2100) relative to the control period (1961–1990)

sequence. Thus changes in temperature related to say a decrease in summer rainfall are determined and used to modify the direct temperature change accordingly. Further details of parameter adjustment for future climate change scenarios, and validation of the CRU-WG in reproducing RCM projected changes are provided by Kilsby et al. (2007) and Jones et al. (2009). The CRU-WG was thus conditioned using the simulated future daily rainfall series for Eindhoven for the 2071–2100 time-slice (described in Section 5.1) to generate temporally consistent daily series of weather variables, perturbed in accordance with individual RCM projections of change.

Before examining the projected changes a validation of the CRU-WG, perturbation was undertaken to assess whether the means of the simulated temperature series reliably represent the additive application of the CFs as indicated by Eq. 4. To test the simulated future temperature series, the mean daily temperature simulated by the CRU-WG is compared with that which would be expected through the additive application of the relevant rebased RCM CFs directly to the CRU-WG simulated control climate means (T_{EXP}). The CRU-WG simulated control climate means were demonstrated to be a robust simulation of the observations in Section 4.2 and so this process represents an appropriate assessment of the application of the CFs. Figure 9 shows that, for each RCM, T_{EXP} lies within the two standard deviations of CRU-WG FUT for most half-monthly periods and demonstrates that the difference between the control and future downscaled temperature series reproduces the changes in mean temperature projected by the RCMs.

An examination of the changes in CRU-WG FUT derived from Fig. 9 indicates that they are consistent with the RCM CFs; the largest changes in mean temperature are simulated during late summer with the increase for August in the range of +3.3°C (REMO_H) to +7.7°C (RCAO_E). The smallest increases are projected during spring, for example the change for April ranges from +2.0°C (ARPEGE_H) to +3.8°C (RCAO_E). For all months except January the largest increase in the ensemble is projected by the two ECHAM4-driven RCMs; this sensitivity being greatest during spring and high summer. Consequently the range of projected mean summer (JJA) temperatures ranges from 19.9°C (REMO_H) to 23.3°C (RCAO_E) whilst for winter (DJF) the range is from 7.7°C (ARPEGE_H) to 9.1°C (RCAO_E) relative to simulated means for the *WObs* period of 16.8°C and 3.8°C respectively.

The range of future projections of *TN*, *T*, *TX* and PET derived from the ensemble of RCM experiments are summarised in Fig. 10. Greater sensitivity of temperatures is seen in the simulations using CFs derived from the ECHAM4-driven RCMs, particularly during summer months and for *TX*. Consequently, the mean monthly ensemble range for projected change in *TX* is 4.1°C in summer compared with a 1.9°C range in winter. For *TN* the range is 3.1°C and 2.0°C in summer and winter respectively.

Changes in simulated future PET (Fig. 10) are strongly related to the corresponding temperature change in each RCM and consequently the largest changes are projected by RCAO_E. Mean annual PET is projected to increase for all models, from 663 mm/year simulated for the *WObs* period to values ranging from 777 mm/year (+17%; ARPEGE_H) and 904 mm/year (+36%; RCAO_E) with large increases of up to +49% (RCAO_E) during summer months.

For many sectors the greatest impact of climate change is likely to be associated with extreme events and it is therefore important to test the ability of a model to adequately represent the occurrence of such events and not just the average behaviour. The change in occurrence of extremes was examined using four standard tempera-

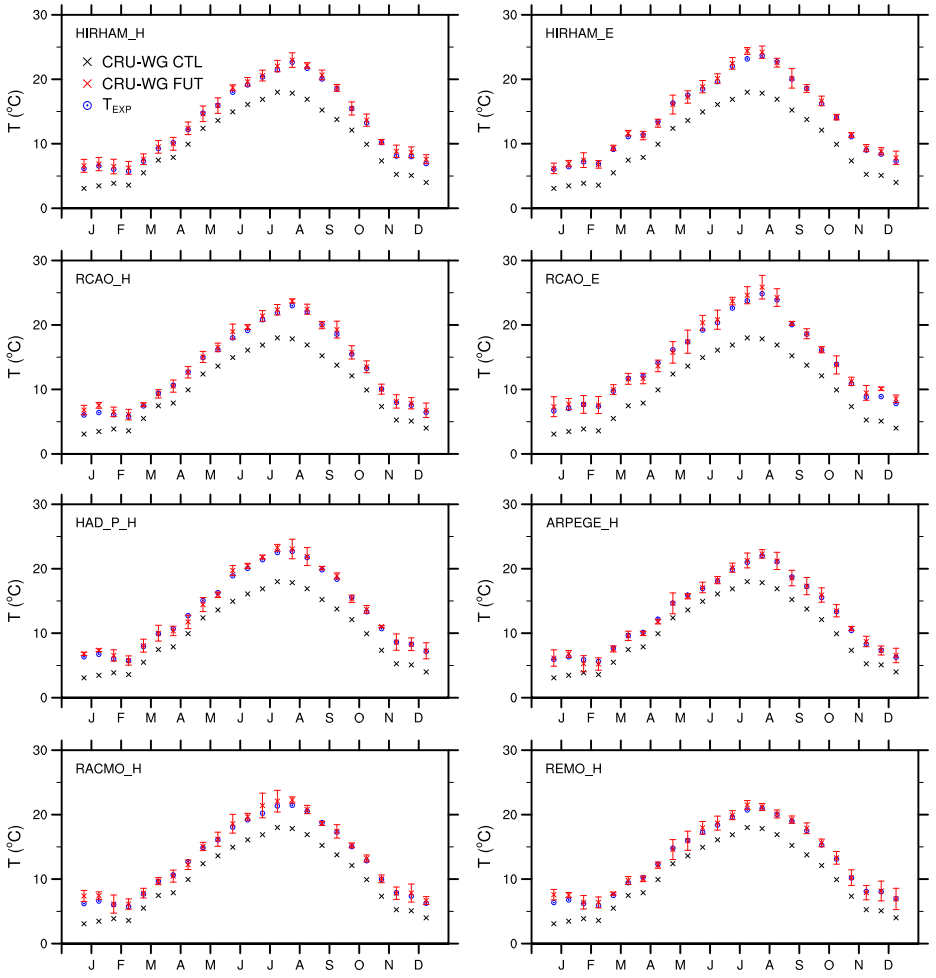

Fig. 9 Validation of future mean monthly temperature for each of the eight 100-year Climatic Research Unit weather generator (CRU-WG) simulations for the 2071–2100 time-slice. The *lower crosses* denote the simulated CRU-WG means for the weather observation period 1985–2006 (CRU-WG CTL and the circles denote the expected future half-monthly means (T_{EXP}). The *upper crosses* indicate the CRU-WG simulated future mean temperatures (CRU-WG FUT) with the error bars representing variability denoted by two standard deviations of the simulated 100 annual means

ture indices (Table 6). The 10th and 90th percentiles of the observed daily minimum and maximum temperature distribution were calculated for each half-month and were used to define thresholds for the corresponding periods within each series simulated by the CRU-WG. First, an additional validation was undertaken of the simulations for the *WObs* period by calculating the accumulated seasonal totals for each index and comparing these with the observed frequencies (Fig. 11). For most seasons the CRU-WG captures the observed distributions reasonably well, particularly for TN. The observed frequency of "warm nights" (TN90) totals are well reproduced throughout the year though the number of "cold nights" (TN10)

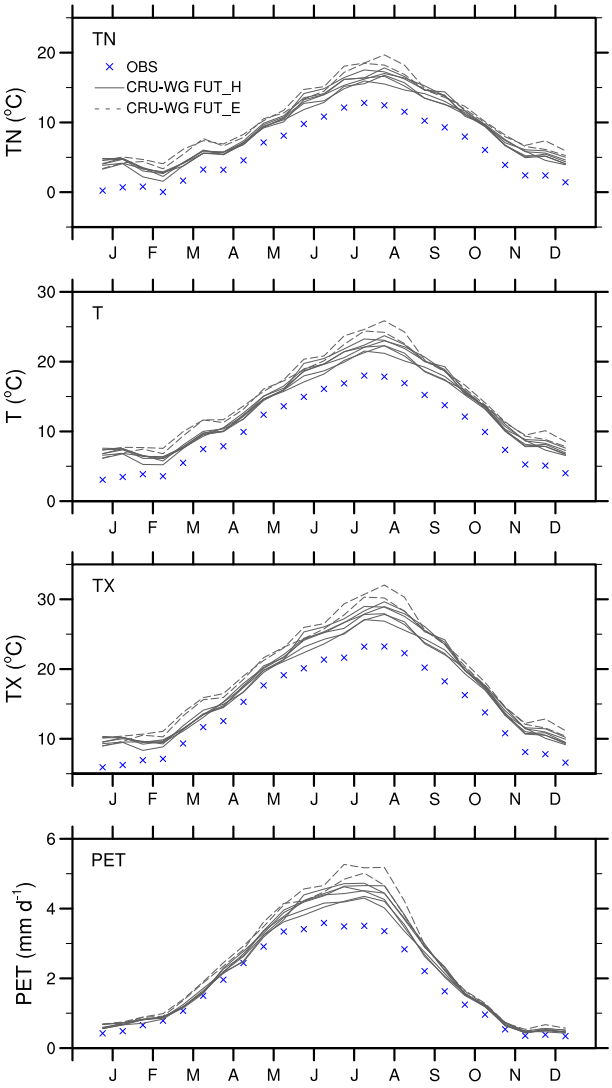

Fig. 10 Future mean daily temperature minima (TN), mean (T) and maxima (TX) and potential evapotranspiration (PET) for the 2071–2100 time-slice simulated by the Climatic Research Unit weather generator (CRU-WG). The *lower crosses* denote the means for the weather observation period (1985–2006; OBS), the *grey lines* show the half-monthly means for the individual simulations corresponding to the eight Regional Climate Model (RCM) experiments. The two *dashed lines* denote the simulations using RCMs driven by the ECHAM4 General Circulation Model (CRU-WG FUT_E) whilst the *solid lines* denote the simulations using RCMs driven by the HadAM3H General Circulation Model (CRU-WG FUT_H)

Table 6 List of extreme indices used to validate the Climatic Research Unit weather generator (CRU-WG)

Index	Definition
TN10	Number of days below 10th percentile daily minimum temperature calculated for each half month for the period of observations (*WObs*; 1985–2006)
TX10	As for TN10 but for daily maximum temperature
TN90	Number of days exceeding 90th percentile daily minimum temperature calculated for each half month for the period of observations
TX90	As for TN90 but for daily maximum temperature

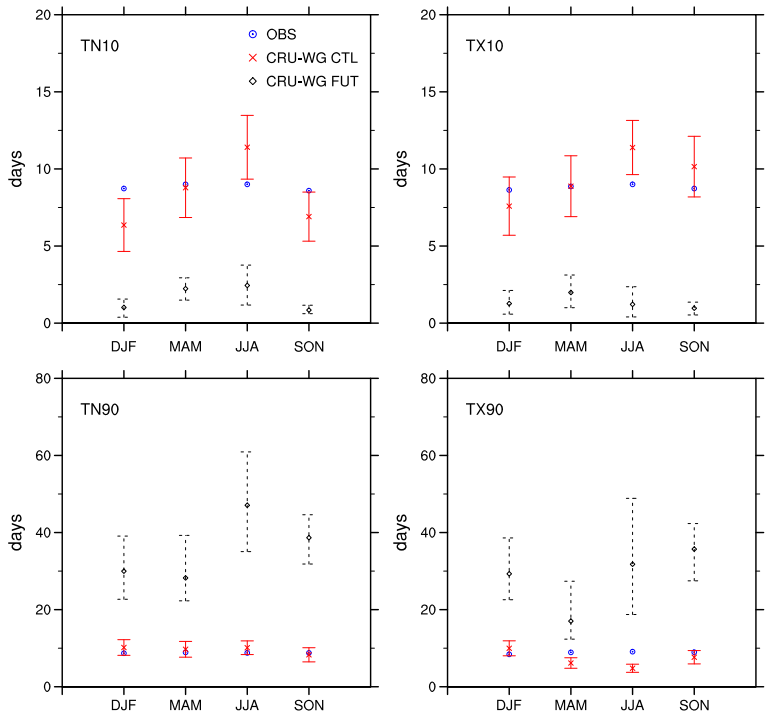

Fig. 11 Comparison of seasonal total daily temperature extremes TN10, TX10, TN90 and TX90 as defined by each of the four indices given in Table 6. The *circles* denote the observed totals (OBS). The *crosses* indicate the totals simulated by the Climatic Research Unit weather generator (CRU-WG) for the weather observation (1985–2006) period (CRU-WG CTL) with the associated *error bars* showing two standard deviations of the estimated annual variability in CRU-WG simulations. The *diamonds* indicate the ensemble mean values for the eight CRU-WG downscaled future scenarios for 2071–2100 (CRU-WG FUT) with the error bars providing the ensemble minimum and maximum

is underestimated in winter. The largest difference is apparent in the number of "hot days" (TX90) which is underestimated during spring and summer indicating that the frequency of extreme hot periods may not be reproduced in the simulated series.

Calculating the frequencies with which each percentile threshold was exceeded in the future scenarios indicates that whilst there is considerable uncertainty in the magnitude of the change in occurrence of extreme events, the projections indicate a climate with less (more) frequent cold (warm) extremes throughout the year at Eindhoven. In particular, there is a large projected increase in the frequency of TN90 events during summer, with the ensemble mean indicating a fourfold increase relative to the control period. However, the uncertainty in projections of TN90 and TX90 events is also large, for example, for summer TN90 ranges from 35 days per year (REMO_H) to 60 days per year (RCAO_E). Since the CRU-WG underestimates the frequency of TX90 events in the control period it is very likely that these events will become much more frequent by the end of the century, likely at or exceeding the upper end of the projected range shown in Fig. 11.

6 Discussion and conclusion

In this paper we describe a method to produce a downscaled multi-model ensemble of daily multi-site rainfall scenarios for the Dommel catchment and consistent representative temperature and potential evapotranspiration scenarios for hydrological impact assessment in the Dommel catchment. An integrated application of the CF approach applied to a stochastic spatial–temporal rainfall model in combination with a rainfall conditioned weather generator was used to produce statistically downscaled climate change scenarios for different RCM experiments. Validation of the stochastic STNSRP model and CRU-WG indicated that both produce reliable simulations of the current climate and, with the exception of summer maxima, the CRU-WG simulates extreme temperatures reasonably well. Although this relatively poor performance for extreme summer temperatures highlights a need for future development of the weather generator, the resultant simulations may still be used to provide an assessment of relative future change in climate and hydrology dependent upon the application and sensitivity of the analysis to the underestimation of summer extremes at a daily resolution. Jones et al. (2009) suggest that improvements in the simulation of extremes might be achieved through the use of more complex statistical distributions, although the perturbation of additional coefficients for future scenarios is not a trivial matter. It should also be noted that climate models themselves do not simulate the blocking atmospheric regimes that lead to such events well (Blenkinsop et al. 2009; Murphy et al. 2009). Overall, considering the combined skill demonstrated by the STNSRP model and the CRU-WG, the approach is considered a suitable means to provide downscaled climate change scenarios for hydrological modelling of the Dommel and is the first time that the CF-weather generator approach of Kilsby et al. (2007) has been extended for use with a spatial–temporal rainfall generator. In addition to downscaling for the 22 raingauges' locations the STNSRP model's spatial process provides the potential to downscale at arbitrary locations other than at rain gauges used for calibration. It should also be noted that the combined CF, rainfall model and weather generator downscaling methodology (Kilsby et al. 2007), and by extension the approach described here, surmounts a number of shortcomings of the traditional perturbation approach. The combined methodology used here in general produces simulated future rainfall time series with different occurrence patterns, moments, and persistence properties than the control series, observations or climate model outputs. The development of such statistical downscaling tools is important if the use of probabilistic methods in impact assessments is to become more widespread as proposed by Collins (2007).

Here, future daily precipitation for the Dommel catchment is projected to exhibit a spatially averaged increase of +9% to +40% during winter for 2071–2100 relative to 1961–1990. In summer, mean daily precipitation is projected to decrease on average by 16% to 57%. Temperature is projected to increase throughout the year with the greatest increase during summer, although the range of projections is also largest during summer (from 3.1°C to 6.5°C). These changes are consistent with the regional projections for the whole PRUDENCE ensemble summarised by Christensen and Christensen (2007). The daily weather generator simulations also indicate an increase in the frequency of extreme temperatures, though again there is considerable uncertainty in the magnitude of the change. Potential evapotranspiration is projected to increase by +17% to +36% on a mean annual basis, with largest increases during summer months (e.g. +21% to +49% during July).

Although the ensemble of RCM experiments shows consistency in the direction of seasonal changes, the individual experiments diverge in terms of the magnitude of projected changes in daily precipitation, temperature and potential evapotranspiration. In addition, the downscaled climate change projections for the Dommel catchment are also strongly influenced by the GCM used to provide boundary conditions for each RCM experiment. This is consistent with previous analyses of temperature and precipitation change (e.g. Déqué et al. 2007; Fowler et al. 2007b) and has been shown to be an important factor in the assessment of projected changes in impacts (Dankers and Feyen 2009; Kay et al. 2009; Manning et al. 2009). A multi-model ensemble of climate change scenarios based on different RCMs and GCMs thus provides robust estimates of precipitation, temperature and evapotranspiration for hydrological impact assessments in this, or indeed any, region. However, it should be noted that the PRUDENCE ensemble does not fully represent structural uncertainty in climate models, particularly as only two GCMs were used in the ensemble, and the GCM-RCM matrix is not fully explored, constituting an 'ensemble of opportunity'. Secondly, the future projections in this ensemble are limited to the SRES A2 emissions (medium–high) scenario (Nakićenović et al. 2000) as PRUDENCE only provides a limited number of RCM simulations for the SRES B2 emissions (medium–low) scenario. Within PRUDENCE the uncertainty derived from the limited choice of emissions scenario is greatest for summer temperatures over southern Europe (Déqué et al. 2007) where the use of other scenarios is recommended. Furthermore, incomplete knowledge of atmospheric processes and the inability to resolve fine-scale physics necessitates the parameterization of key processes and properties, such as convection, cloud formation and cloud characteristics. Consequently, the full range of model uncertainty can only be quantified when used alongside perturbed physics ensembles (Tebaldi and Knutti 2007) which fully explore the range of model parameterizations. A truly comprehensive assessment of uncertainty should take into account the "cascade of uncertainty" referred to by Schneider (1983), for e.g. incorporating uncertainty arising from the future response of biogeochemical cycles and from the trajectory of emissions. However, in demonstrating the application of these downscaling methods, they could, with the appropriate resources, be extended to the full range of PRUDENCE outputs and to additional state-of-the-art RCM experiments such as those provided by the ENSEMBLES[1] project.

This framework, using a spatially coherent stochastic rainfall model and a weather generator, both perturbed by projected changes from climate models, provides a significant advance in the ability to provide an assessment of the uncertainty of the impacts of climate change on small to medium-scale catchments (50 km^2–2000 km^2). Considering potential future hydrological impacts for the Dommel, the projected increase in daily mean precipitation and proportion of wet days during winter may result in higher seasonal discharges, with a possible increase in the leaching of heavy metals and nutrients towards surface water. In addition, the projected decrease in mean daily precipitation and strong increase in potential evapotranspiration during summer months is expected to lower summer discharges, possibly with an associated increase in the frequency and intensity of hydrological droughts. It has been demonstrated that during droughts water quality in the Meuse deteriorates,

[1] http://ensembles-eu.metoffice.com/

for example, due to increased concentrations of major elements and some heavy metals (van Vliet and Zwolsman 2008). The scenarios created here are therefore being used to generate hydrological simulations to assess the potential impact of climate change on heavy metal contamination of the Dommel catchment (Visser et al. 2011) and the rainfall scenarios have been used to assess the impact of climate change on a groundwater influenced hillslope ecosystem (Brolsma et al. 2010). This demonstrates how the approach outlined here may be used as a stepping stone towards a probabilistic assessment of future hydrological responses to climate change in this region. It also provides projections which can be used to make robust adaptation and mitigation decisions with regards to the future impacts of climate change.

Acknowledgements This research was financially supported by the European Commission FP6 Integrated Project AquaTerra (Project no. 505428) under the thematic priority sustainable development, global change and ecosystems. Dr. Hayley Fowler was supported by a NERC Postdoctoral Fellowship award (2006–2010) NE/D009588/1. RCM data were obtained from the FP5 PRUDENCE project archive (http://prudence.dmi.dk/) which was supported by EU contract EVk2-CT2001-00132. We would like to thank Rudmer Jilderda of the Royal Netherlands Meteorological Institute (KNMI) and Marc Christiaens of the Royal Meteorological Institute of Belgium (KMI-RMI) for providing precipitation, temperature and evapotranspiration data of the Dutch and Belgian part of the study area.

Appendix 1: Pattern scaling

The global mean temperature (μ) projected for each GCM integration is calculated from GCM output from the IPCC data distribution centre[2] for 30-year time-slices centred on the years 1975 (control), 2025, 2055 and 2085 (future) which we will denote as μ^G_{Con}, μ^G_{2025}, μ^G_{2055} and μ^G_{Fut} (where G indicates the GCM from which the temperature is derived). Linear interpolation of μ^G_{Con} and μ^G_{2055} was used to estimate the GCM projected global mean temperature for 1995, the central year of the weather observation ($WObs$) period (1985–2006), which we write as μ^G_{Wobs}. Following the approach described in Burton et al. (2010a) the future estimate of temperature variance, $TV_i^{R,Est}$, for RCM R and month i may be calculated from the observed value, TV_i^{WObs}, by rebasing the change factor as:

$$TV_i^{R,Est} = \frac{\alpha^R_{TV,i}}{1 + \left(\alpha^R_{TV,i} - 1\right) SF^{G(R)}_{WObs}} \, TV_i^{WObs} \tag{5}$$

where the change factors are as calculated in Eq. 1 and the scale factor for the observation period, $SF^{G(R)}_{WObs}$, may be calculated from the GCM conditioning the RCM R, $G(R)$, as:

$$SF^{G(R)}_{WObs} = \frac{\mu^{G(R)}_{WObs} - \mu^{G(R)}_{Con}}{\mu^{G(R)}_{Fut} - \mu^{G(R)}_{Con}} \tag{6}$$

Here we note that the equivalent expression to Eq. 5 for a rebased additive change factor approach to estimate future mean daily temperature from the available

[2] http://www.ipcc-data.org/

observations, T_i^{WObs}, may be written as shown in Eq. 7, applying the change factors calculated in Eq. 3 and the scale factors derived in Eq. 6:

$$T_i^{R,Est} = \alpha_{T,i}^{R}\left(1 - SF_{WObs}^{G(R)}\right) + T_i^{WObs} \tag{7}$$

References

Barth JAC, Grathwohl P, Fowler HJ, Bellin A, Gerzabek MH, Lair GJ, Barceló D, Petrovic M, Navarro A, Négrel P, Petelet-Giraud E, Darmendrail D, Rijnaarts H, Langenhoff A, De Weert J, Slob A, Van Der Zaan BM, Gerritse J, Frank E, Gutierrez A, Kretzschmar R, Gocht T, Steidle D, Garrido F, Jones KC, Meijer S, Moeckel C, Marsman A, Klaver G, Vogel T, Bürger C, Kolditz O, Broers HP, Baran N, Joziasse J, Von Tümpling W, Van Gaans P, Merly C, Chapman A, Brouyère S, Batlle Aguilar J, Orban Ph, Tas N, Smidt H (2009) Mobility, turnover and storage of pollutants in soils, sediments and waters: achievements and results of the EU project AquaTerra. A review. Agron Sustain Dev 29:161–173

Blenkinsop S, Fowler HJ (2007) Changes in drought characteristics for Europe projected by the PRUDENCE regional climate models. Int J Climatol 27:1595–1610

Blenkinsop S, Jones PD, Dorling SR, Osborn TJ (2009) Observed and modelled influence of atmospheric circulation on Central England Temperature extremes. Int J Climatol 29:1642–1660

Booij MJ (2005) Impact of climate change on river flooding assessed with different spatial model resolutions. J Hydrol 303:176–198

Brolsma RJ, van Vliet MTH, Bierkens MFP (2010) Climate change impact on a groundwater-influenced hillslope ecosystem. Water Resour Res 46(11):W11503. doi:10.1029/2009WR008782

Burton A, Kilsby CG, Fowler HJ, Cowpertwait PSP, O'Connell PE (2008) RainSim: a spatial temporal stochastic rainfall modelling system. Environ Model Softw 23:1356–1369

Burton A, Fowler HJ, Blenkinsop S, Kilsby CG (2010a) Downscaling transient climate change using a Neyman–Scott Rectangular Pulses stochastic rainfall model. J Hydrol 381(1–2):18–32. doi:10.1016/j.jhydrol.2009.10.031

Burton A, Fowler HJ, Kilsby CG, O'Connell PE (2010b) A stochastic model for the spatial–temporal simulation of nonhomogeneous rainfall occurrence and amounts. Water Resour Res 46:W11501. doi:10.1029/2009WR008884

Cannon AJ (2008) Probabilistic multisite precipitation downscaling by an expanded Bernoulli–Gamma density network. J Hydrometeorol 9(6):1284–1300. doi:10.1175/2008JHM960.1

Charles SP, Bates BC, Smith IN, Hughes JP (2004) Statistical downscaling of daily precipitation from observed and modelled atmospheric fields. Hydrol Process 18:1373–1394. doi:10.1002/hyp.1418

Christensen JH, Christensen OB (2007) A summary of the PRUDENCE model projections of changes in European climate by the end of this century. Clim Change 81(Supplement 1):7–30

Christensen JH, Carter TR, Rummukainen M, Amanatidis G (2007) Evaluating the performance and utility of regional climate models: the PRUDENCE project. Clim Change 81(Supplement 1):1–6

Collins M (2007) Ensembles and probabilities: a new era in the prediction of climate change. Philos Trans R Soc A 365:1957–1970

Conway D, Jones PD (1998) The use of weather types and air flow indices for GCM downscaling. J Hydrol 213:348–361

Cowpertwait PSP (1995) A generalized spatial–temporal model of rainfall based on a clustered point process. Proc R Soc Lond A 450:163–175

Cowpertwait PSP (1998) A Poisson-cluster model of rainfall: high-order moments and extreme values. Proc R Soc Lond A 454:885–898

Dankers R, Feyen L (2009) Flood hazard in Europe in an ensemble of regional climate scenarios. J Geophys Res 114:D16108. doi:10.1029/2008JD011523

Déqué M, Rowell DP, Lüthi D, Giorgi F, Christensen JH, Rockel B, Jacob D, Kjellström E, de Castro M, van den Hurk B (2007) An intercomparison of regional climate simulations for Europe: assessing uncertainties in model projections. Clim Change 81:53–70

De Jonge M, de Vijver BV, Blust R, Bervoets L (2008) Responses of aquatic organisms to metal pollution in a lowland river in Flanders: a comparison of diatoms and macroinvertebrates. Sci Total Environ 407:615–629

De Wit MJM, van den Hurk B, Warmerdam PMM, Torfs PJJF, Roulin E, van Deursen WPA (2007) Impact of climate change on low-flows in the river Meuse. Clim Change 82:351–372
Diaz-Nieto J, Wilby RL (2005) A comparison of statistical downscaling and climate change factor methods: impacts on low flows in the River Thames, United Kingdom. Clim Change 69:245–268
FAO (1986) Irrigation water management: irrigation water needs. FAO, Rome
Fowler HJ, Kilsby CG, O'Connell PE, Burton A (2005) A weather-type conditioned multi-site stochastic rainfall model for the generation of scenarios of climatic variability and change. J Hydrol 308(1–4):50–66
Fowler HJ, Blenkinsop S, Tebaldi C (2007a) Linking climate change modelling to impacts studies: recent advances in downscaling techniques for hydrological modelling. Int J Climatol 27:1547–1578
Fowler HJ, Ekström M, Blenkinsop S, Smith AP (2007b) Estimating change in extreme European precipitation using a multimodel ensemble. J Geophys Res 112:D18104. doi:10.1029/2007JD008619
Gellens D, Roulin E (1998) Streamflow response of Belgian catchments to IPCC climate change scenarios. J Hydrol 210:242–258
Gupta VK, Waymire E (1979) A stochastic kinematic study of subsynoptic space–time rainfall. Water Resour Res 15:637–644
Haylock MR, Cawley GC, Harpham C, Wilby RL, Goodess CM (2006) Downscaling heavy precipitation over the United Kingdom: a comparison of dynamical and statistical methods and their future scenarios. Int J Climatol 26:1397–1415
Jacob D, Bärring L, Christensen OB, Christensen JH, de Castro M, Déqué M, Giorgi F, Hagemann S, Hirschi M, Jones R, Kjellström E, Lenderink G, Rockel B, Sánchez E, Schär C, Seneviratne SI, Somot S, van Ulden A, van den Hurk B (2007) An inter-comparison of regional climate models for Europe: model performance in present-day climate. Clim Change 81(Supplement 1):31–52
Jones PD, Salmon M (1995) Development and integration of a stochastic weather generator into a crop growth model for European agriculture. MARS project, final report to Institute of Remote Sensing Applications, Agricultural Information Systems (ISPRA), UK
Jones PD, Kilsby CG, Harpham C, Glenis V, Burton A (2009) UK Climate Projections science report: projections of future daily climate for the UK from the Weather Generator. University Of Newcastle, UK, p 48. ISBN 978-1-906360-06-1
Kay AL, Davies HN, Bell VA, Jones RG (2009) Comparison of uncertainty sources for climate change impacts: flood frequency in England. Clim Change 92:41–63
Kilsby CG, Jones PD, Burton A, Ford AC, Fowler HJ, Harpham C, James P, Smith A, Wilby RL (2007) A daily weather generator for use in climate change studies. Environ Model Softw 22:1705–1719
Le Cam LM (1961) A stochastic description of precipitation. In: Neyman J (ed) Proceedings of the fourth Berkeley symposium on mathematical statistics and probability, vol 3. University of California, Berkeley, California, pp 165–186
Leander R, Buishand TA (2007) Resampling of regional climate model output for the simulation of extreme river flows. J Hydrol 351:331–343
Leander R, Buishand TA, Aalders P, de Wit MJM (2005) Estimation of extreme floods of the River Meuse using a stochastic weather generator and a rainfall–runoff model. Hydrol Sci J 50(6):1089–1102
Leander R, Buishand TA, van den Hurk BJJM, de Wit MJM (2008) Estimated changes in flood quantiles of the river Meuse from resampling of regional climate model output. J Hydrol 351:331–343
Lenderink G, van Ulden A, van den Hurk B, Keller F (2007) A study on combining global and regional climate model results for generating climate scenarios of temperature and precipitation for the Netherlands. Clim Dyn 29:157–176
Manning LJ, Hall JW, Fowler HJ, Kilsby CG (2009) Using probabilistic climate change information from a multi-model ensemble for water resources assessment. Water Resour Res 45:W11411. doi:10.1029/2007WR006674
Mitchell TD (2003) Pattern scaling: an examination of the accuracy of the technique for describing future climates. Clim Change 60:217–242
Murphy JM, Sexton DMH, Jenkins GJ, Boorman PM, Booth BBB, Brown CC, Clark RT, Collins M, Harris GR, Kendon EJ, Betts RA, Brown SJ, Howard TP, Humphrey KA, McCarthy MP, McDonald RE, Stephens A, Wallace C, Warren R, Wilby R, Wood RA (2009) UK climate projections science report: climate change projections. Met Office Hadley Centre, Exeter
Nakićenović N, Alcamo J, Davis G, de Vries HJM, Fenhann J, Gaffin S, Gregory K, Grubler A, Jung TY, Kram T, La Rovere EL, Michaelis L, Mori S, Morita T, Papper W, Pitcher H, Price L, Riahi K, Roehrl A, Rogner H-H, Sankovski A, Schlesinger M, Shukla P, Smith S, Swart R, van Rooijen

S, Victor N, Dadi Z (2000) Emissions Scenarios. A Special Report of Working Group III of the Intergovernmental Panel on Climate Change, Cambridge University Press, Cambridge, p 559
Palutikof JP, Goodess CM, Watkins SJ, Holt T (2002) Generating rainfall and temperature scenarios at multiple sites: examples from the Mediterranean. J Clim 15:3529–3548
Pieterse NM, Bleuten W, Jørgensen SE (2003) Contribution of point sources and diffuse sources to nitrogen and phosphorus loads in lowland river tributaries. J Hydrol 271:213–225
Pope VD, Gallani ML, Rowntree PR, Stratton RA (2000) The impact of new physical parametrizations in the Hadley Centre climate model: HadAM3. Clim Dyn 16:123–146
Prudhomme C, Reynard N, Crooks S (2002) Downscaling of global climate models for flood frequency analysis: where are we now? Hydrol Process 16:1137–1150
Rodriguez-Iturbe I, Cox DR, Isham V (1987) Some models for rainfall based on stochastic point processes. Proc R Soc Lond A 410:269–288
Roeckner E, Arpe K, Bengtsson L, Christoph M, Claussen M, Dümenil L, Esch M, Giorgetta M, Schlese U, Schulzweida U (1996) The atmospheric general circulation model ECHAM-4: model description and simulation of present-day climate. Report No 218, Max-Planck Institute for Meteorology, Hamburg, Germany, p 90
Santer BD, Wigley TML, Schlesinger ME, Mitchell JFB (1990) Developing climate scenarios from equilibrium GCM results. Report No 47, Max-Planck-Institut für Meteorologie, Hamburg, p 29
Schneider SH (1983) CO_2, climate and society: a brief overview. In: Chen RS, Boulding E, Schneider SH (eds) Social science research and climate change: in interdisciplinary appraisal. D Reidel, Boston, MA, USA, pp 9–15
Semenov MA, Barrow EM (1997) Use of a stochastic weather generator in the development of climate change scenarios. Clim Chang 35:397–414
Tebaldi C, Knutti R (2007) The use of the multi-model ensemble in probabilistic climate projections. Philos Trans R Soc A 365:2053–2075
Tebaldi C, Nychka D, Mearns LO (2004) From global mean responses to regional signals of climate change: simple pattern scaling, its limitations (or lack of) and the uncertainty in its results In: Proceedings of the 17th conference on probability and statistics in the atmospheric sciences, AMS Annual Meeting, Seattle, WA
van den Hurk B, Klein Tank A, Lenderink G, van Oldenborg G, Katsman C, van den Brink H, Keller F, Bessembinder J, Burgers G, Komen G, Hazeleger W, Drijfhout S, van Ulden A (2006) Climate Change Scenarios 2006 for The Netherlands. KNMI Scientific Report WR 2006-01, KNMI, The Netherlands
van Pelt SC, Kabat P, ter Maat H, van den Hurk BJJM, Weerts AH (2009) Discharge simulations performed with a hydrological model using bias corrected regional climate model input. Hydrol Earth Syst Sci 13:2387–2397
van Vliet MTH, Zwolsman JJG (2008) Impact of summer droughts on the water quality of the Meuse river. J Hydrol 353:1–17. doi:10.1016/j.jhydrol.2008.01.001
Visser A, Kroes J, van Vliet MTH, Blenkinsop S, Fowler HJ, Broers HP (2011) Climate change impacts on the leaching of a heavy metal contamination in a small lowland catchment. J Contam Hydrol. doi:10.1016/j.jconhyd.2011.04.007
Watts M, Goodess CM, Jones PD (2004a) The CRU daily weather generator. BETWIXT Technical Briefing Note 1, Version 2, February 2004
Watts M, Goodess CM, Jones PD (2004b) Validation of the CRU daily weather generator. BETWIXT Technical Briefing Note 4, Version 1, June 2004
Wilby RL (1999) The weather generation game: a review of stochastic weather models. Prog Phys Geogr 23:329–357
Wilby RL, Wigley TML (1997) Downscaling general circulation model output: a review of methods and limitations. Prog Phys Geogr 21:530–548
Wilby RL, Dawson CW, Barrow EM (2002) SDSM—a decision support tool for the assessment of regional climate change impacts. Environ Model Softw 17:145–157